

# The COOH-Terminal Domain of FLI-1 Is Necessary for Full Tumorigenesis and Transcriptional Modulation by EWS/FLI-1<sup>1,2</sup>

Afsane Arvand, Scott M. Welford, Michael A. Teitell, and Christopher T. Denny<sup>3</sup>

Department of Experimental Pathology and Laboratory Medicine [A. A., M. A. T.], Molecular Biology Institute [S. M. W., M. A. T., C. T. D.], Jonsson Comprehensive Cancer Center [M. A. T., C. T. D.], and Department of Pediatrics, Gwynne Hazen Cherry Memorial Labs [C. T. D.], University of California at Los Angeles, Los Angeles, California 90095

## ABSTRACT

More than 85% of Ewing's family tumors carry a specific chromosomal translocation that fuses the NH<sub>2</sub> terminus of the *EWS* gene to the COOH terminus of the *FLI1* transcription factor. It has been shown previously that both the transactivation domain encoded by *EWS* and the DNA binding domain of *FLI1* were necessary for transforming cells to anchorage independence. We now report that a COOH-terminal domain in addition to the *FLI1* DNA binding domain is necessary to promote cellular transformation. NIH 3T3 cells expressing a COOH-terminal deletion mutant (EWS/*FLI1* ΔC) have a greatly reduced capability to form colonies in soft agar and tumors in severe combined immunodeficient mice. The rate of tumor formation for NIH 3T3 that express EWS/*FLI1* ΔC is 50 days, whereas EWS/*FLI1* forms tumors within 22 days. In addition, cells expressing the EWS/*FLI1* ΔC mutant failed to completely demonstrate the round-cell histology that is seen in both Ewing's tumor cell lines and NIH 3T3 cells expressing full-length EWS/*FLI1*. Northern and microarray analyses were performed to assess the effect of loss of the *FLI1* COOH terminus on transcriptional modulation of EWS/*FLI1* target genes. We found that although EWS/*FLI1* ΔC up-regulates smaller numbers of genes (21 genes) compared with EWS/*FLI1* (34 genes), 41% of the EWS/*FLI1* targets were also up-regulated by EWS/*FLI1* ΔC. On the other hand, EWS/*FLI1* ΔC is unable to down-regulate genes (3 genes) as efficiently as EWS/*FLI1* (39 genes) with only one target gene repressed by both fusion constructs. Our study indicates that the EWS/*FLI1* transcription factor has strong transcriptional activating as well as repressing properties and suggests that transcriptional activation and repression of target genes may occur through biochemically different mechanisms.

## INTRODUCTION

ES<sup>4</sup> and PNETs demonstrate examples of specific chromosomal translocations associated with unique classes of malignancy. In the vast majority of cases, ES/PNETs contain genomic rearrangements that fuse the NH<sub>2</sub> terminus of *EWS* to the COOH terminus of one of five potential *ETS* proteins. Individually both *EWS* and *ETS* genes have transcriptional regulatory roles in normal mammalian physiology. *EWS* is a RNA-binding protein that is structurally and functionally related to *TLS/FUS* and *TAFII68* (1, 2). *ETS* genes encode for a family of transcription factors that are defined by a highly conserved 85-amino-acid domain, which mediates site-specific binding to DNA. Although there is variability in the precise fusion points between *EWS* and partner *ETS* genes, the *ETS* DBD domain and the *EWS* transac-

tivation domain are invariably included in all ES/PNET EWS/*ETS* fusions.

*EWS/FLI1* is the most prevalent fusion and is found in ~85% of ES/PNET patients (3, 4). Alternative and less frequent *EWS* fusion partners in ES/PNET include: *ERG* on chromosome 21 q22.2, *ETV1/ER81* on chromosome 7 p22, *E1AF/PEA3* on chromosome 17 q12, and *FEV* on chromosome 2 (5–8). *ES/PNET* fusion genes can be subdivided into two groups according to amino acid sequence similarity in their *ETS* DBDs. EWS/*FLI1*, EWS/*ERG*, and EWS/*FEV* form one highly related group (Group 1). EWS/*ETV1* and EWS/*E1AF* form the second group (Group 2).

Extensive experimental data exist that demonstrate the oncogenic potential of *EWS/ETS* fusion genes from both groups. Expression of EWS/*ETS* proteins promote anchorage-independent growth *in vitro* and/or accelerate tumorigenesis of NIH 3T3 cells *in vivo* (9–11). The transforming activities of EWS/*FLI1* require both the *EWS* and the DBD of *FLI1* (12–14). Antagonizing EWS/*FLI1* through antisense oligonucleotides or dominant negative *FLI1* constructs inhibits growth of ES/PNET tumor-derived cell lines both *in vitro* and *in vivo* (15–20). These data, together with the observation that *EWS* fusion genes and fusion proteins are present in virtually all Ewing's cases, provide strong evidence that formation of *EWS/ETS* chimeric fusion gene is a necessary event in the development of ES/PNET.

Recently, we have shown that NIH 3T3 cells that express EWS/*FLI1* or EWS/*ETV1* form tumors in immunodeficient mice that display a round-cell histology reminiscent of ES/PNET (11). This result suggests that despite their structural differences, Group 1 and Group 2 EWS/*ETS* fusions both promote tumorigenesis through similar genetic pathways. However, there appears to be a quantitative difference in tumorigenic potential between these two EWS/*ETS* fusion types: EWS/*FLI1* was able to induce tumor formation at a significantly faster rate than EWS/*ETV1*. Surprisingly, initial experiments suggested that the enhanced tumorigenic effect of EWS/*FLI1* mapped to the COOH-terminal 89-amino-acids of *FLI1* rather than the *FLI1* DBD (11).

This present work extends this initial finding and demonstrates crucial biological roles of the *ETS* COOH-terminal domain in *EWS/ETS* fusion genes. We show that the loss of the COOH-terminal domain greatly attenuates the ability of EWS/*FLI1* to promote anchorage-independent growth. Cells that express EWS/*FLI1* COOH-terminal deletion mutants demonstrate a progressive decrease in tumorigenic potency and loss of round-cell histology. Finally, deletion of the *FLI1* COOH terminus profoundly effects transcriptional repression of specific *EWS/FLI1* target genes.

## MATERIALS AND METHODS

### Construction of Retroviral Expression Vectors for FEF ΔC, and FEF ΔC Derivatives

We defined FEF amino acids 386–409 as region 1, amino acids 410–444 as region 2, and 445–474 as region 3. FEF ΔC was created by PCR amplification of the parental FEF (type 4). We used a 5' primer that contained an *EcoRI* restriction site, Flag sequence, and the first 20 bp of the *EWS* coding region; and a 3' primer that matched the sequence of the last 30 bp found at the

Received 1/31/01; accepted 4/26/01.

The costs of publication of this article were defrayed in part by the payment of page charges. This article must therefore be hereby marked *advertisement* in accordance with 18 U.S.C. Section 1734 solely to indicate this fact.

<sup>1</sup> Supported by NIH Grant CA32737 from the National Cancer Institute; by Training Grant CA09056 (to A. A.); by USPHS National Research Service Award GM07185 (to S. M. W.); by NIH Grant CA74929 (to M. A. T.); and by the Lymphoma Research Foundation of America.

<sup>2</sup> Supplementary data for this article is available at *Cancer Research* Online [http://cancerres.aacrjournals.org].

<sup>3</sup> To whom requests for reprints should be addressed, at UCLA Medical Center, Department of Pediatrics, A2-312 MDCC, Los Angeles, CA 90095.

<sup>4</sup> The abbreviations used are: ES, Ewing's sarcoma; PNET, primitive neuroectodermal tumor; DBD, DNA binding domain; SCID, severe combined immunodeficient; FEF, Flag-tagged EWS/*FlI-1*.

end of the FLI1 DBD, followed by a *Hind*III site. Constructs FEF  $\Delta$ 3, and FEF  $\Delta$ (2+3) were made the same way, using the same 5' primer, but with 3' primers matching the last 20 bp of region 2 in the COOH terminus, or the last 20 bp of region 1, respectively. Constructs FEF  $\Delta$ 1, FEF  $\Delta$ 2, FEF  $\Delta$ (1+2), and FEF  $\Delta$ (1+3) were created using a two-stage PCR process. In the first step, two fragments were amplified. The first fragment, a 5' EWS/FLI1  $\Delta$  C fragment, was amplified as described above. The second fragment was created by using complementary 3' PCR primers to specific regions in the COOH terminus and corresponding 5' primer for that region. These two PCR fragments were then joined by amplifying them in a reaction using vector-specific primers that flanked EWS and the FLI1 sequences. All of our 3' primers contained a *Hind*III restriction sites. The PCR products were then digested with *Eco*RI and *Hind*III, gel purified, and subcloned into the retroviral expression vector SR $\alpha$  MSV-tkneo  $\Delta$ *Hind*III. The inserts were then subcloned into pBluescript II KS+ and sequenced.

### Retrovirus Production and Cell Culture

For production of retroviruses, we used 293T cells. Cells were cultured in DMEM supplemented with 5% calf serum and glutamine. 293Ts were transfected with recombinant SR $\alpha$  MSV-Tk Neo expression vectors and  $\psi(-)$  packaging plasmids by the calcium phosphate precipitation method. After 48 h, the media containing the retrovirus were harvested. Infections were carried out by adding the recombinant viral stocks to polyclonal NIH 3T3 cells; the infected cells were then selected with 450  $\mu$ g of G418 per ml of culture media for 7–10 days.

The monoclonal cell lines were created by using a limiting dilution protocol. In brief, cells were seeded in 96-well culture plates at 5 cells/ml or 0.5 cells/ml, and fed with conditioned media from the parental lines. Wells containing single clones were expanded to establish the cell lines. Tumor-derived cell lines were established by plating minced tumors in DMEM/10% calf serum.

### Growth in Semisolid Media and Tumorigenesis Assay

Five  $\times 10^3$  polyclonal NIH 3T3 cells expressing FEF, FEF  $\Delta$ C, and empty vector (Tk Neo) were seeded in semisolid agar as described previously (12), photographs were taken at day 14. One million NIH 3T3 cells that had been selected for the FEF, FEF  $\Delta$ C, and FEF  $\Delta$ C deletion constructs were s.c. injected into the nape region of the neck of CB17 SCID mice. All of the mice were female and of about 5–6 weeks of age at the time of injection. Mice were observed until a grossly visible tumor of 2 cm in diameter was present. The animals were killed at this time, and the tumors were excised; a small piece of the tumor was fixed in 10% buffered formalin for paraffin embedding and H&E staining.

### Northern and Western Blot Analyses

RNA and protein were harvested from infected cells immediately after antibiotic selection. Total RNA was prepared from lysates using STAT-60 (TEL-TEST, Inc.),  $\sim 8 \mu$ g of RNA of each sample was electrophoresed in a formaldehyde-1% gel, and transferred to nitrocellulose membrane by standard methods. Northern blot hybridization and probe preparations were carried through as described previously (12). For immunoblots, cells were harvested and lysed in NP40 lysis buffer (50 mM Tris, 300 mM NaCl, 10% glycerol, 1 mM EDTA). Protein concentration was determined by Bradford assay against BSA standards. Sixty  $\mu$ g of protein in SDS loading buffer was loaded for each cell line, Coomassie Blue staining of the SDS gel, and Ponceau S staining of the nitrocellulose membrane after transfer was used to assess equal loading. Monoclonal anti-Flag (M2) was obtained from Sigma Chemical Co. The secondary antibody was horseradish peroxidase-conjugated goat-antimouse (Jackson Labs). The antibody-bound proteins were detected with ECL (Enhanced ChemiLuminescence) Western blotting detection reagents (Amersham).

### Affymetrix Genechip Analysis

**Genechips.** Mu11kSubA Genechips were purchased from Affymetrix, Inc. The Mu11kSubA set contains  $\sim 6500$  probe sets from mRNA transcripts and EST clusters. Oligonucleotide probes are synthesized on the arrays complementary to a portion of each gene. On the murine 11K set, there are  $\sim 20$  oligonucleotide probe pairs for each sequence.

**Preparation of Biotin-labeled cRNA for Hybridization.** NIH 3T3 cells were virally infected with corresponding retroviral stocks FEF, FEF  $\Delta$ C, and Tk Neo in two independent experiments. Biotin-labeled cRNA was prepared according to Affymetrix protocols. Briefly, total RNA was isolated from NIH 3T3 cells expressing FEF, FEF  $\Delta$ C, and empty vector (Tk Neo) from experiments 1 and 2 according to the RNeasy total RNA isolation protocol (Qiagen). Twenty  $\mu$ g of the total RNA were used to synthesize first-strand cDNA (Life Technologies, Inc.). T7-(dT)<sub>24</sub> oligomer [5'-GGCCAGTGAATTGTAATAC-GACTCACTATAGGGAGGCGG-(dT)<sub>24</sub>-3'] (Ambion MEGAScript T7 kit) was used for priming first-strand cDNA synthesis instead of the oligo (dT), second-strand cDNA was synthesized according to standard protocols. Biotin-11-cytidine-5'-triphosphate (Bio-11-CTP;ENZO) and Biotin-16-Uridine-5'-triphosphate (Bio-16-UTP;ENZO) were then incorporated in an *in vitro* transcription reaction using T7 polymerase (Ambion MEGAScript T7 kit Cat. No.1334). Murine Genechips were hybridized with Biotin-labeled cRNA probes from each replicate experiment at the University of California, San Diego, GeneChip Core facility. The biotin-labeled probes were bound to R-phycoerythrin streptavidin (Molecular Probes P/N S-866), and scanned on Hewlett Packard GeneArray scanner. The results were analyzed using GeneSpring software (Silicon Genetics, Inc.). We defined a threshold of 20 for the negative and low values (31, 32). Only genes that scored P (present) call on both replicates as foreground signals were considered in the computation analyses. The averages of intensities for all experiments were then calculated and were used to determine fold differences. In our analyses, we also compared the duplicates to each other. For example, when the level of expression of all genes in FEF  $\Delta$ C experiment 1 were compared with FEF  $\Delta$ C experiment 2, we found that 5.6% of the genes are different from each other by at least 2-fold in their intensity values. This difference was less in the two Tk Neo trials (3.2%), and more in the FEF duplicates (8.2%). Therefore, we felt justified to compute a simple intensity average for each gene, and report only the genes that are up- or down-regulated by 3-fold or more (Supplementary Table 1 and 2 can be viewed online at <http://cancerres.aacrjournals.org>). Furthermore, we defined a second criteria for uniquely modulated genes: these genes must be up- or down-regulated by 3-fold compared with Tk Neo, and the difference between FEF and FEF  $\Delta$ C must be at least 2-fold. For example, a gene is considered uniquely up-regulated by FEF when FEF/TK is equal or more than three and FEF/FEF  $\Delta$ C is more than 2-fold (Supplementary tables).

## RESULTS

**FLI1 COOH Terminus Is Necessary for Efficient EWS/FLI1-induced NIH 3T3 Anchorage-independent Growth and Tumorigenesis.** Sequence comparison of EWS/FLI1 and EWS/ETV1 demonstrates that their COOH termini are the most divergent domains between these two fusion molecules (Fig. 1). Whereas the FLI1 and ETV1 ETS DBDs are only 63% identical, both of these DBDs can bind the same consensus sequence *in vitro* (6, 21). The ETV1 DBD

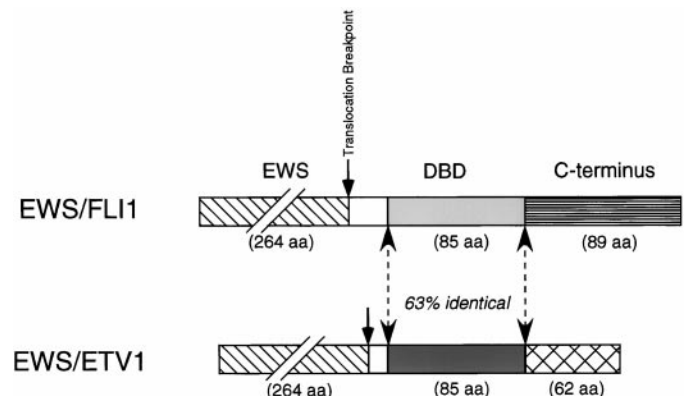


Fig. 1. Schematic representation of *EWS/FLI1* (type 4) and *EWS/ETV1* fusion genes. The regions in *EWS/FLI1* are as follows: ▨, EWS amino acids 1–264; □, FLI1 37 amino acids at the translocation breakpoint; ■, FLI1 DBD; ▩, FLI1 COOH terminus. The regions in *EWS/ETV1* are depicted as: ▨, EWS amino acids 1–264; □, 17 amino acids of ETV1 at the translocation breakpoint; ■, ETV DBD; ▩, ETV1 COOH terminus.

can also replace the biological activity of the FLI1 DBD in transformation assays (11). On the contrary, the COOH terminus of ETV1 is significantly shorter than the COOH terminus of FLI1, and, more importantly, it does not share any substantial homology with the FLI1 COOH terminus.

To directly demonstrate potential biological roles of the COOH terminus, a NH<sub>2</sub>-terminal Flag-tagged EWS/FLI1 fusion protein with amino acids 386–474 deleted (FEF ΔC) was created, and its ability to transform cells was assessed in comparison to the full-length Flag-tagged EWS/FLI1 (FEF). The FEF ΔC construct does not contain the last 89 amino acids after the FLI1 ETS DNA-binding domain. Polyclonal NIH 3T3 populations that express FEF ΔC were generated by retroviral-mediated gene transfer (FEF ΔC-3T3). As an initial indication of biological activity, FEF ΔC-3T3 cells were plated in soft agar, and their growth compared with similar NIH 3T3 cell populations expressing full-length FEF or empty vector control (Tk Neo; Fig. 2A). FEF ΔC-3T3 cells exhibit markedly attenuated anchorage-independent growth, forming ~90% fewer colonies in soft agar than cells expressing FEF.

To further investigate the tumorigenic requirement of the FLI1 COOH terminus, the tumor-forming potency of FEF ΔC-3T3 cells

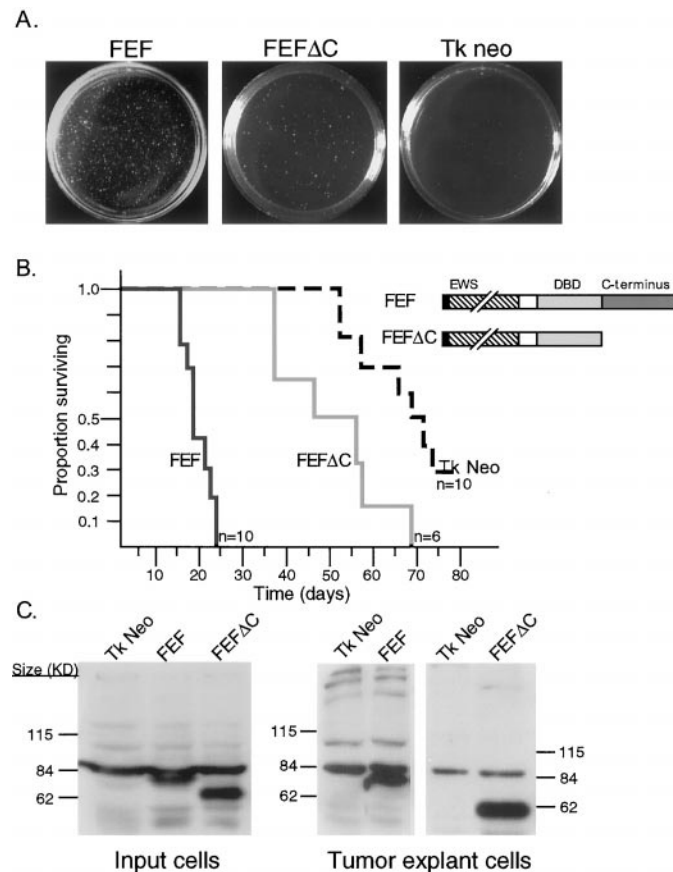


Fig. 2. A, effect of FEF ΔC on anchorage independent growth of NIH 3T3 cells in soft agar. Cells were plated at low density in soft agar and photographed 2 weeks later. Representative agar assay images show formation of macroscopic colonies in the full-length FEF plate but not in FEF ΔC. Under standard conditions, the parental cell line containing empty vector (Tk Neo) does not form colonies in semisolid media. B, survival plot comparing survival among mice given injections of FEF, FEF ΔC, and empty vector. This survival curve shows the percentage of mice that do not have a tumor of 2-cm diameter after a certain number of days after injection of the cells. *Solid black line*, mice injected with NIH 3T3 FEF; *gray line*, FEF ΔC mice; *dashed line*, Tk Neo negative control. C, immunoblot analyses of FEF and FEF ΔC expression in infected NIH 3T3 cells from input and explant tumor cell lines. NP40 whole-cell extracts were separated on SDS-PAGE, and FEF and FEF ΔC were detected with an anti-Flag antibody. A background band migrating at  $M_r \sim 84,000$  is seen in all of the NIH 3T3 cell lysates. *KD*, in thousands.

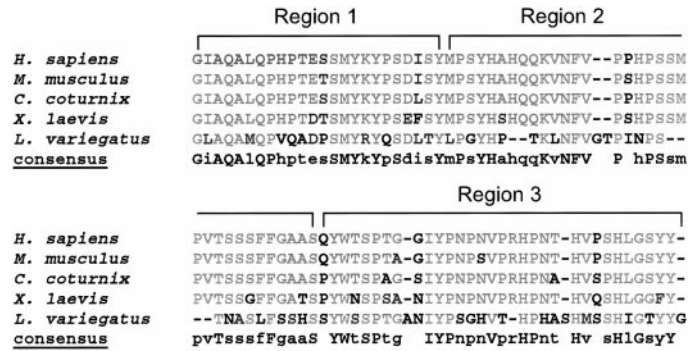


Fig. 3. Alignment of COOH-terminal regions of FLI1 across four species. *Region 1*, FEF amino acids 386–409; *Region 2*, amino acids 410–444; *Region 3*, amino acids 445–474.

was also assessed *in vivo*. Equal numbers of NIH 3T3 cells expressing FEF, FEF ΔC, or empty vector were injected s.c. into CB-17-SCID mice. The rate of tumor formation for tumors of 2.0 cm in diameter was monitored over a 90-day period. Although cells expressing either mutant or wild-type FEF constructs all form tumors, the mean time to tumor formation in FEF ΔC-3T3 cells (50 days) differs significantly from that of FEF-3T3 cells (22 days; Fig. 2B).

The protein expression levels of FEF and FEF ΔC in G418 selected cells were confirmed by immunoblotting analyses with anti-Flag antibody (Fig. 2C). The level of FEF ΔC mutant protein detected is approximately equal to the full-length, indicating that loss of the FLI1 COOH terminus does not destabilize EWS/FLI1 protein. To confirm that expression of the FEF ΔC was not lost during the long period to formation of tumor, Western blot analyses was repeated on the tumor cell lines derived from the excised tumors (Fig. 2C). FEF ΔC protein is highly expressed in tumor-derived cell lines, as is full-length FEF. These data indicate that the differences in *in vitro* and *in vivo* behavior of these cell lines are attributable to altered biological characteristics of FEF ΔC and not simply differences in protein expression levels or stability.

**Interstitial Deletions within the FLI1 COOH Terminus Attenuate EWS/FLI1 Tumorigenicity.** Amino acid sequence alignment of the FLI1 COOH terminus shows high homology across diverse species ranging from 97% overall identity between human and mouse to 83% identity between human and *Xenopus laevis* (Fig. 3). In addition to the results of the FEF ΔC transformation assays, this evolutionary conservation across species further suggests the biological importance of this domain.

To see whether the tumor-promoting activity of the FLI1 COOH terminus could be more precisely mapped, a series of mutants with interstitial deletions in this region was generated. On the basis of sequence alignment, we divided the FLI1 COOH terminus 89 amino acids into three regions (Fig. 3). Six FEF deletion mutants were created that contained all possible combinations of the three subdivided COOH-terminal regions (Fig. 4). These constructs were then transduced into NIH 3T3 cells using replication-deficient retroviruses. Polyclonal NIH 3T3 populations were then injected s.c. into SCID mice and the time to tumor formation was assessed.

All NIH 3T3 populations that express FEF mutants with COOH-terminal interstitial deletions form tumors (Fig. 4). Attenuation of tumorigenicity was incremental and generally paralleled the amount of the COOH terminus that was deleted rather than the absence of any particular region. For example, mutants containing a deletion of any single COOH terminus region (FEF Δ1, FEF Δ2, or FEF Δ3) form tumors at the same rate as full-length FEF. Mutants with deletions of two COOH-terminal regions form tumors at rates that are intermediate

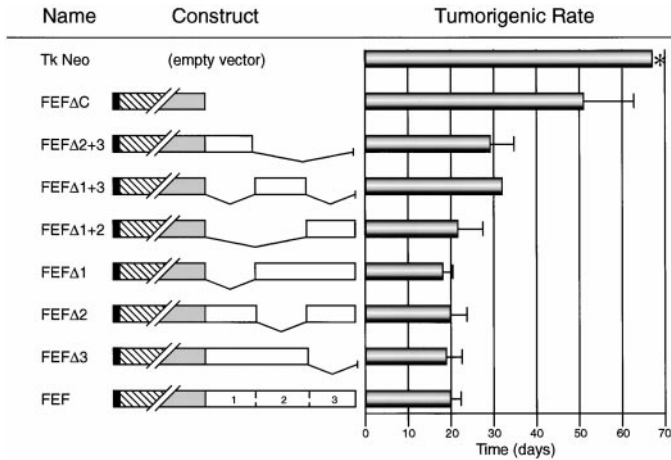


Fig. 4. Structures of FEF deletion mutants lacking all or parts of the COOH terminal of FLI1. Rates of tumor formation of the respective deletions and control cell lines are summarized in histogram form. ■, Flag tag; ▨, EWS amino acids 1–264 present in EWS/FLI1 (type 4); ▩, FLI1 DBD; □, FLI1 COOH terminus regions 1, 2, and 3. (\*), not all of the Tk Neo control mice formed tumors; these mice were killed at 90 days without a tumor.

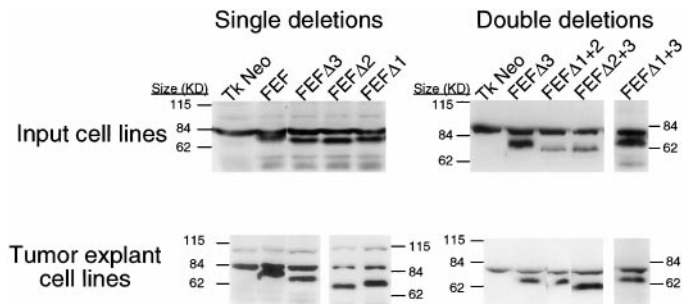


Fig. 5. Immunoblot analyses of the expression of FEF COOH-terminal deletion mutants in infected NIH 3T3 cells and tumor explant cell lines. Whole-cell extracts were fractionated on SDS-PAGE and the mutant proteins were detected with an anti-Flag antibody. A nonspecific cross-reacting background band of  $M_r \sim 84,000$  is again seen in all of the lysates. *KD*,  $M_r$  in thousands.

between full-length FEF and FEF  $\Delta C$ . As before, expression levels of FEF interstitial mutants were assessed in input cell lines and tumor explant cell lines by anti-Flag immunoblot (Fig. 5). Protein levels of all of the mutants were comparable with full-length FEF, which indicated that the observed differences in tumorigenic rates among NIH 3T3 populations are attributable to differing biological properties of the EWS/FLI1 COOH-terminal interstitial mutants.

**Loss of FLI1 COOH Terminus in EWS/FLI1 Alters NIH 3T3 Tumor Morphology.** We have previously shown that NIH 3T3 cells expressing EWS/ETS fusions form tumors that are histologically distinct from the spindle cell histology that is typical of NIH 3T3 fibroblast-derived tumors (22). The finding that the COOH terminus of FLI1 is important for efficient induction of tumorigenesis by EWS/FLI1 suggests that this domain might also play a role in dictating round-cell morphology.

Histological analyses were performed on the tumors generated from NIH 3T3 cells stably expressing complete or partial FEF COOH-terminal mutants to investigate what effect the COOH terminus has on tumor cell morphology. Control cell lines, containing either empty vector (Tk Neo) or full-length FEF, displayed the expected morphologies: empty vector tumor cells were densely packed and spindle shaped, creating the appearance of fibrosarcoma; FEF cells displayed a round-cell appearance reminiscent of ES/PNET (Fig. 6A). All of the FEF mutants with partial deletions of the COOH terminus also demonstrated small-round-cell histology (data not shown). By contrast,

complete deletion of the COOH terminus (FEF  $\Delta C$ ) promoted tumors that displayed biphenotypic morphology with both round and spindle components (Fig. 6A). This biphenotypic appearance was recapitulated in culture of FEF  $\Delta C$  tumor-derived cell lines (data not shown).

The presence of a mixed population of cells suggests that either (a) there is sufficient cell to cell variation in the expression of FEF  $\Delta C$  to give rise to two morphologies or (b) there are genetically distinct subpopulations of NIH 3T3 cells that can respond differently to FEF  $\Delta C$ . To discern between these two possibilities, monoclonal NIH 3T3 cell lines expressing full-length FEF, FEF  $\Delta C$ , or control empty vector were isolated by limiting dilution. We tested two FEF and TK Neo monoclonal and eight monoclonal of  $\Delta C$ . Monoclonal were then implanted into SCID mice and the resultant tumors examined histologically. Both the full-length FEF and empty vector monoclonal tumors maintained their native pure morphologies. FEF monoclonal lead to round-cell tumors, and empty vector to spindle-cell tumors, consistent with the parental polyclonal populations tested in the same assay (data not shown). The FEF  $\Delta C$  monoclonal tumors, however, were split. Of the five FEF  $\Delta C$  monoclonal that formed tumors within the duration of the assay, four displayed round-cell morphologies (e.g., Fig. 6A, FEF  $\Delta C$  monoclonal 1), whereas one formed spindle-cell tumors (Fig. 6A, FEF  $\Delta C$  monoclonal 2). There appears to be no correlation between the rate of tumor formation and the histological appearance of these tumors. Anti-Flag immunoblot demonstrates equal levels of FEF  $\Delta C$  protein in spindle-compared with round-cell tumor cell lines, which indicates that the difference in tumor-cell

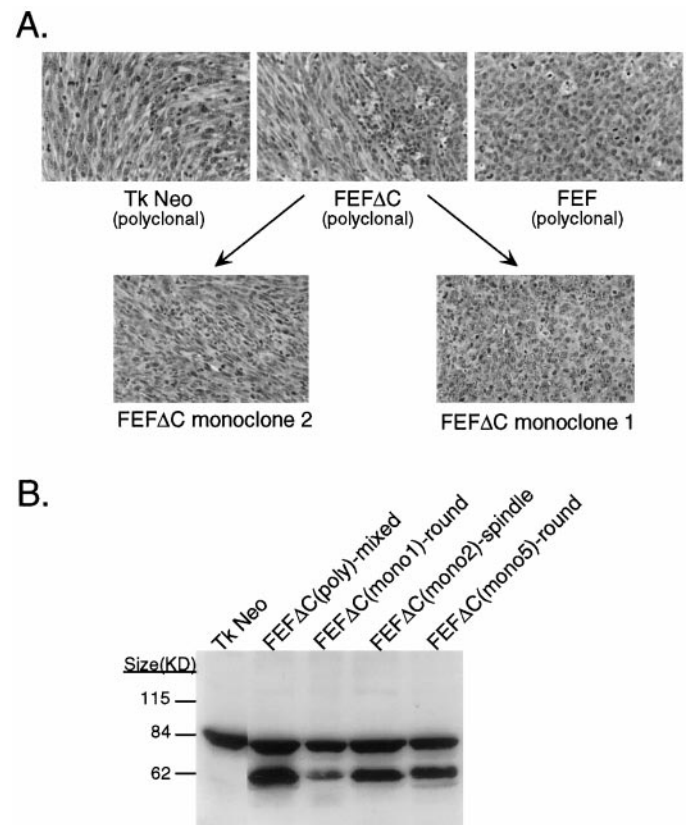


Fig. 6. A, FEF  $\Delta C$  induces tumors with a biphenotypic morphology. Cells expressing FEF, FEF  $\Delta C$ , and Tk Neo were injected s.c. into SCID mice, and excised tumors were formalin fixed, paraffin embedded, sectioned, and stained with H&E. Photomicrographs of tumor sections are shown ( $\times 200$  and  $\times 400$ ). Both elongated spindle cells and ES-like small round cells are present in the polyclonal  $\Delta C$  tumor. Representative histology sections from two  $\Delta C$  monoclonal tumors with distinct morphology are presented.  $\Delta C$  monoclonal 1, 4, and 5 displayed only round-cell morphology, whereas monoclonal 2 showed pure spindle-like morphology. B, immunoblot analysis of the expression of FEF  $\Delta C$  protein in the tumor-derived polyclonal and monoclonal cell lines.

morphology was not attributable to variation in FEF  $\Delta C$  expression (Fig. 6B).

**Mutation of the FLI1 COOH Terminus Alters the EWS/FLI1 Target Gene Repertoire.** EWS/FLI1 is thought to mediate its oncogenic effect by acting as a transcription factor that modulates the expression of a set of target genes. The fact that the FEF  $\Delta C$  mutant has attenuated tumorigenic potency and altered histological appearance suggests that FEF  $\Delta C$  may not be able to regulate target genes as effectively as full-length FEF.

Northern analyses were performed to provide an initial estimate of the effect of deleting the FLI1 COOH terminus on the transcriptional activation of selected FEF target genes. Total RNA Northern blots generated from polyclonal NIH 3T3 populations stably expressing each of the FEF mutants were hybridized to cDNA probes from five previously described FEF up-regulated target genes (Refs. 10, 23–25; Fig. 7). In general, the FEF-deletion mutants similarly modulated all five genes that were up-regulated by full-length FEF. Although the FEF mutants were not able to up-regulate target genes to as high a level as full-length FEF, most target genes were induced to levels above empty vector negative control (Tk Neo). FEF  $\Delta(2+3)$ , containing only region 1 of the COOH terminus, proved the exception because it was unable to transcriptionally activate three of the five FEF target genes. These results suggest that although the FEF mutants have decreased tumorigenic potencies, they are for the most part still able to transcriptionally activate EWS/FLI1 target genes.

Whereas the Northern experiments seemed to demonstrate a trend, they represented a small number of potential target genes. To perform a broader comparison of genes that are transcriptionally modulated by FEF versus FEF  $\Delta C$ , microarray studies were performed. Heterogeneous-labeled cRNA probes were generated from polyclonal NIH 3T3 cells expressing full-length FEF, FEF  $\Delta C$ , and empty vector, and were hybridized to prefabricated oligonucleotide arrays representing 6500 murine genes (Affymetrix-Mu11KsubA). Expression levels of each of the 6500 genes in the NIH 3T3 populations were quantified by the intensity of hybridization on the microarrays. Genes that were mod-

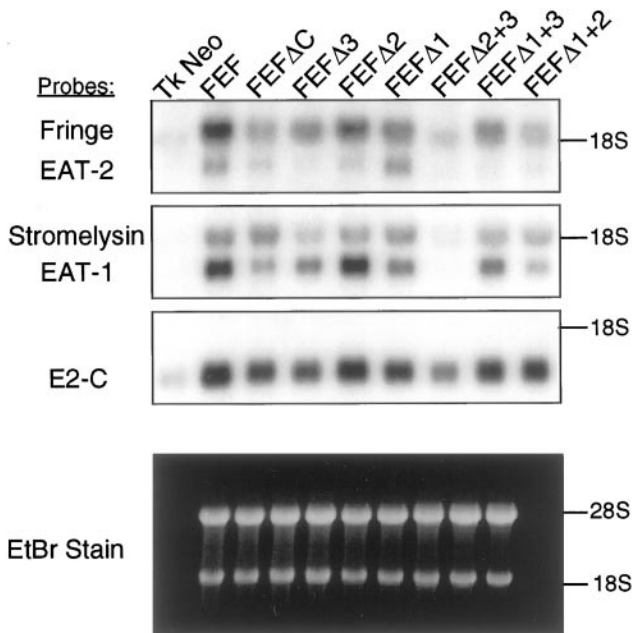


Fig. 7. Top three panels, Northern analyses of FEF target genes in NIH 3T3 cells expressing Tk Neo, FEF, FEF  $\Delta C$ , and FEF  $\Delta C$  mutants. Expressions of all five target genes are repressed in cells expressing  $\Delta C$ , or the  $\Delta C$  mutants compared with FEF. Bottom panel, ethidium bromide (EtBr) staining of RNA gel depicting equal loading of the RNA samples for the Northern blot analyses.

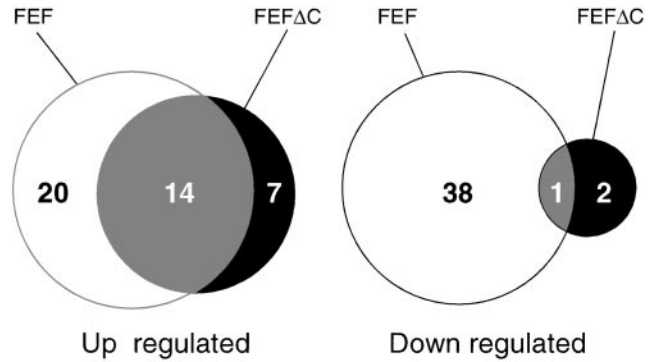


Fig. 8. FEF  $\Delta C$  is a less potent transcriptional repressor than FEF. Venn diagrams depict gene regulation by FEF  $\Delta C$  and FEF as measured by microarray analysis. A unique up-regulated gene in FEF is defined as FEF/Tk $\geq$ 3 and FEF/FEF  $\Delta C$  $\geq$ 2. Shared up-regulated genes depicted in the overlapping regions are defined as FEF/Tk $\geq$ 3, FEF  $\Delta C$ /Tk $\geq$ 3, and FEF/FEF  $\Delta C$ <2. The reciprocal relationships hold for down-regulated genes. (For more details, see “Materials and Methods.”) FEF  $\Delta C$  up-regulates 41% of FEF activated genes over Tk Neo, but represses only 2.5% of down-regulated genes.

ulated >3-fold by either FEF or FEF  $\Delta C$  over empty vector control were identified and compared (Fig. 8). The Genechip analyses are the average of two independent experiments (see “Material and Methods” for details). Each cRNA probe was prepared twice from two freshly transduced NIH 3T3 cell populations and hybridized onto two Affymetrix chips from the same murine 11KsubA set. As an internal control for our Genechip analysis, we evaluated the level of activation of known EWS/FLI1 target genes. *mFNG* and murine *E2-C*, two previously identified target genes, were present in the Mu11ksubA gene set. In our analyses, we identified both of these genes to be activated >2-fold by FEF. Although FEF  $\Delta C$  also activated *mFNG* and *E2-C*, activation was lower than with full-length FEF, which matched our Northern blot analysis (Fig. 7).

Genechip analyses demonstrated that the EWS/FLI1 (FEF) transcription factor had both strong transcriptional activating as well as strong repressing properties, and that the FLI1 COOH terminus is involved mainly in target gene down-regulation. We have identified genes that are differentially expressed by a factor of three or greater compared with empty vector (Tk Neo). Our analysis shows that FEF  $\Delta C$  up-regulated smaller numbers of genes (21 genes) compared with FEF (34 genes), but the overlap between the two populations is significant. Fourteen (41%) of FEF-activated genes were also activated by FEF  $\Delta C$ . By contrast, the cohort of down-regulated genes presents a very different picture. Whereas FEF down-regulated 39 genes by 3-fold, FEF  $\Delta C$  down-regulated only 3 genes. More significantly, only 1 (2.5%) of the genes repressed by FEF was also down-regulated by FEF  $\Delta C$  (Fig. 8). It should be noted that because these experiments used stable expressing cell lines, the observed down-regulated target genes could have resulted either from direct repression by EWS/FLI1 or indirectly through activation of a repressor(s) by EWS/FLI1.

## DISCUSSION

We have demonstrated that the COOH terminus of FLI1 plays a crucial functional role in EWS/FLI1 oncogenicity. It is necessary both for promotion of NIH 3T3 cell anchorage independent growth and for acceleration of tumor formation in SCID mice. Despite these profound effects, we were unable to localize these biological activities to a subdomain within the 89-amino-acid COOH terminus. Interstitial mutation analyses showed that EWS/FLI1 fusions containing any of the FLI1 COOH-terminal subdomains promote tumorigenesis better than the construct that lacks the COOH terminus entirely. It appears

that there may not be a minimal domain within the COOH terminus to which we can assign distinct functions and that the FLI1 COOH terminus contains a large functional domain that can remain biologically intact amid the deletions we have made. Thus, a deletion in part of a specific region changes the activity to some degree, but it does not abrogate activity in our assay entirely.

One possible explanation is that any stretch of amino acids after the DBD can rescue the transforming ability of FEF  $\Delta$ C, perhaps by altering the secondary structure of the entire protein. However, artificial replacement of the FLI1 COOH terminus by the COOH terminus of ETV1 resulted in a chimeric protein (EWS/FLI/ETV) that demonstrated the same attenuated NIH 3T3 tumor formation as that seen with FEF  $\Delta$ C (11). These observations strongly suggest that the specific FLI1 COOH-terminal sequence contains a unique biological function necessary for efficient cellular transformation.

In addition to tumor rate, the loss of pure-round-cell histology in FEF  $\Delta$ C-3T3 tumors provides another indication of biological activity associated with the FLI1 COOH terminus. We have shown previously that this histology is not attributable simply to rapid tumor growth but has been seen in virtually all of our EWS/ETS NIH 3T3 tumor assays. The biphenotypic spindle/round-cell morphology seen with FEF  $\Delta$ C tumors can be separated into the two histological components via clonal isolation and is not related to the level of FEF  $\Delta$ C protein expression. This suggests that the differing morphologies are caused by clonal variation within the polyclonal NIH 3T3 populations. We hypothesize that the round-cell morphology requires modulation of a specific set of target genes by the EWS/FLI1 oncoprotein. Full-length FEF can activate all of these genes, irrespective of the variation in the NIH 3T3 genetic background. However, FEF  $\Delta$ C may activate only a subset of these required genes and, therefore, requires a preexisting genetic background to establish the round-cell morphology. An alternative explanation would be that because of the attenuated biology of FEF  $\Delta$ C, additional mutations need to occur subsequent to transduction of the fusion in order for the round-cell morphology to be apparent. Because this morphology is strikingly close to that seen in human ES/PNET, these differing FEF  $\Delta$ C monoclonal lines may prove useful reagents to identify those genes dictating ES/PNET histology.

Although the COOH terminus of FLI1 clearly conveys biological activity to the EWS/FLI1 fusion, the biochemical mechanisms responsible for this effect are presently unclear. One potential explanation is that the COOH terminus plays a role in site-specific DNA binding of EWS/FLI1. However, it has been previously demonstrated that the *in vitro* DNA binding activity of FLI1 with a truncated COOH terminus does not differ from full-length FLI1 (16), and the sequence-specific DNA binding properties of the constructs similar to those with FEF  $\Delta$ C are not different from their wild-type counterparts *in vitro* (1, 26). Nevertheless, equivalency in DNA binding between full-length FEF and FEF  $\Delta$ C may not hold true *in vivo*. ETS proteins are known to form heteromeric complexes with other DNA-binding transcription factors at promoter and enhancer elements of target genes (reviewed in Ref. 27). For example, synergistic interactions have been described between ETS1 and PAX5 at the *MB-1* promoter (28). Interaction with core binding factor (CBF  $\alpha$ 2) has been shown to enhance *in vivo* DNA binding of ETS1 (29). It is possible that the FLI1 COOH terminus mediates interaction with other transcription factors that would enhance binding to regulatory regions of *EWS/FLI1* target genes.

Alternatively, the FLI1 COOH terminus may act to enhance transcriptional activation of *EWS/FLI1* target genes. Previous studies using model reporter gene assays have detected some transcriptional activation properties associated with both the FLI1 and ERG C-termini (1, 26, 30). These results were confirmed in similar assays using  $\beta$ -galactosidase/FLI1 fusion genes (16). The incremental loss of biological activity seen in our partial COOH-terminal deletion mu-

nants is reminiscent of transcriptional activation domains. To a certain extent, the fact that FEF is able to up-regulate some target genes to a higher level than that seen with FEF  $\Delta$ C could be a reflection of loss of transcription activation capability in the COOH terminus.

Our microarray experiments indicate that deletion of the COOH terminus results in a global reduction of genes that are transcriptionally modulated by EWS/FLI1. Not only are the total number of affected target genes reduced but the quantitative degree to which they are modulated is also decreased. Strikingly, this effect is not evenly distributed over up- and down-regulated target genes. Whereas FEF  $\Delta$ C is able to up-regulate up to 41% of the activated genes, it represses only 2.5% of the FEF down-regulated genes. These analyses were performed using a factor of three to determine the differential expression of genes. Interestingly, when we reduced the stringency of the screening to 2-fold, we observed a similar trend (data not shown). On the one hand, this may be simply a fortuitous finding and reflect a differential effect on *EWS/FLI1* target genes involved in mediating gene repression. On the other hand, it may be that transcriptional activation and repression of target genes by EWS/FLI1 may occur through biochemically different mechanisms. Future identification of *EWS/ETS* direct target genes will help distinguish these two possibilities.

## ACKNOWLEDGMENTS

We thank Steven P. Hebert and Bernadette So for their invaluable technical support.

## REFERENCES

- Ohno, T., Ouchida, M., Lee, L., Gatalica, Z., Rao, V. N., and Reddy, E. S. The *EWS* gene, involved in Ewing family of tumors, malignant melanoma of soft parts and desmoplastic small round cell tumors, codes for an RNA binding protein with novel regulatory domains. *Oncogene*, *9*: 3087–3097, 1994.
- Bertolotti, A., Melot, T., Acker, J., Vigneron, M., Delattre, O., and Tora, L. *EWS*, but not *EWS-FLI-1*, is associated with both TFIID and RNA polymerase II: interactions between two members of the TET family, *EWS* and hTAFII68, and subunits of TFIID and RNA polymerase II complexes. *Mol. Cell. Biol.*, *18*: 1489–1497, 1998.
- Turc-Carel, C., Aurias, A., Mugneret, F., Lizard, S., Sidaner, I., Volk, C., Thiery, J. P., Olschwang, S., Philip, I., Berger, M. P., et al. Chromosomes in Ewing's sarcoma. I. An evaluation of 85 cases of remarkable consistency of t(11;22)(q24;q12). *Cancer Genet. Cytogenet.*, *32*: 229–238, 1988.
- Delattre, O., Zucman, J., Plougastel, B., Desmaziere, C., Melot, T., Peter, M., Kovar, H., Joubert, I., de Jong, P., Rouleau, G., et al. Gene fusion with an ETS DNA-binding domain caused by chromosome translocation in human tumours. *Nature (Lond.)*, *359*: 162–165, 1992.
- Sorensen, P. H., Lessnick, S. L., Lopez-Terrada, D., Liu, X. F., Triche, T. J., and Denny, C. T. A second Ewing's sarcoma translocation, t(21;22), fuses the *EWS* gene to another ETS-family transcription factor, *ERG*. *Nat. Genet.*, *6*: 146–151, 1994.
- Jeon, I. S., Davis, J. N., Braun, B. S., Sublett, J. E., Roussel, M. F., Denny, C. T., and Shapiro, D. N. A variant Ewing's sarcoma translocation (7;22) fuses the *EWS* gene to the *ETS* gene *ETV1*. *Oncogene*, *10*: 1229–1234, 1995.
- Urano, F., Umezawa, A., Hong, W., Kikuchi, H., and Hata, J. A novel chimera gene between *EWS* and *E1A-F*, encoding the adenovirus E1A enhancer-binding protein, in extraosseous Ewing's sarcoma. *Biochem. Biophys. Res. Commun.*, *219*: 608–612, 1996.
- Peter, M., Couturier, J., Pacquement, H., Michon, J., Thomas, G., Magdelenat, H., and Delattre, O. A new member of the ETS family fused to *EWS* in Ewing tumors. *Oncogene*, *14*: 1159–1164, 1997.
- Zinszner, H., Albalat, R., and Ron, D. A novel effector domain from the RNA-binding protein TLS or *EWS* is required for oncogenic transformation by *CHOP*. *Genes Dev.*, *8*: 2513–2526, 1994.
- May, W. A., Arvand, A., Thompson, A. D., Braun, B. S., Wright, M., and Denny, C. T. *EWS/FLI1*-induced manic fringe renders NIH 3T3 cells tumorigenic. *Nat. Genet.*, *17*: 495–497, 1997.
- Thompson, A. D., Teitell, M. A., Arvand, A., and Denny, C. T. Divergent Ewing's sarcoma *EWS/ETS* fusions confer a common tumorigenic phenotype on NIH 3T3 cells. *Oncogene*, *18*: 5506–5513, 1999.
- May, W. A., Gishizky, M. L., Lessnick, S. L., Lunsford, L. B., Lewis, B. C., Delattre, O., Zucman, J., Thomas, G., and Denny, C. T. Ewing sarcoma 11;22 translocation produces a chimeric transcription factor that requires the DNA-binding domain encoded by FLI1 for transformation. *Proc. Natl. Acad. Sci. USA*, *90*: 5752–5756, 1993.
- May, W. A., Lessnick, S. L., Braun, B. S., Klemsz, M., Lewis, B. C., Lunsford, L. B., Hromas, R., and Denny, C. T. The Ewing's sarcoma *EWS/FLI-1* fusion gene encodes a more potent transcriptional activator and is a more powerful transforming gene than *FLI-1*. *Mol. Cell. Biol.*, *13*: 7393–7398, 1993.

14. Lessnick, S. L., Braun, B. S., Denny, C. T., and May, W. A. Multiple domains mediate transformation by the Ewing's sarcoma *EWS/FLI-1* fusion gene. *Oncogene*, *10*: 423–431, 1995.
15. Ouchida, M., Ohno, T., Fujimura, Y., Rao, V. N., and Reddy, E. S. Loss of tumorigenicity of Ewing's sarcoma cells expressing antisense RNA to EWS-fusion transcripts. *Oncogene*, *11*: 1049–1054, 1995.
16. Kovar, H., Aryee, D. N., Jug, G., Henockl, C., Schemper, M., Delattre, O., Thomas, G., and Gadner, H. EWS/FLI-1 antagonists induce growth inhibition of Ewing tumor cells *in vitro*. *Cell Growth Differ.*, *7*: 429–437, 1996.
17. Toretzky, J. A., Connell, Y., Neckers, L., and Bhat, N. K. Inhibition of EWS-FLI-1 fusion protein with antisense oligodeoxynucleotides. *J. Neurooncol.*, *31*: 9–16, 1997.
18. Tanaka, K., Iwakuma, T., Harimaya, K., Sato, H., and Iwamoto, Y. EWS-Flil antisense oligodeoxynucleotide inhibits proliferation of human Ewing's sarcoma and primitive neuroectodermal tumor cells. *J. Clin. Investig.*, *99*: 239–247, 1997.
19. Yi, H., Fujimura, Y., Ouchida, M., Prasad, D. D., Rao, V. N., and Reddy, E. S. Inhibition of apoptosis by normal and aberrant Fli-1 and *erg* proteins involved in human solid tumors and leukemias. *Oncogene*, *14*: 1259–1268, 1997.
20. Hahn, K. B., Cho, K., Lee, C., Im, Y. H., Chang, J., Choi, S. G., Sorensen, P. H., Thiele, C. J., and Kim, S. J. Repression of the gene encoding the TGF- $\beta$  type II receptor is a major target of the EWS-FLI1 oncoprotein [Published erratum appears in *Nat. Genet.*, *23*: 481, 1999]. *Nat. Genet.*, *23*: 222–227, 1999.
21. Mao, X., Miesfeldt, S., Yang, H., Leiden, J. M., and Thompson, C. B. The FLI-1 and chimeric EWS-FLI-1 oncoproteins display similar DNA binding specificities. *J. Biol. Chem.*, *269*: 18216–18222, 1994.
22. Teitell, M. A., Thompson, A. D., Sorensen, P. H., Shimada, H., Triche, T. J., and Denny, C. T. *EWS/ETS* fusion genes induce epithelial and neuroectodermal differentiation in NIH 3T3 fibroblasts. *Lab. Investig.*, *79*: 1535–1543, 1999.
23. Braun, B. S., Frieden, R., Lessnick, S. L., May, W. A., and Denny, C. T. Identification of target genes for the Ewing's sarcoma EWS/FLI fusion protein by representational difference analysis. *Mol. Cell. Biol.*, *15*: 4623–4630, 1995.
24. Thompson, A. D., Braun, B. S., Arvand, A., Stewart, S. D., May, W. A., Chen, E., Korenberg, J., and Denny, C. EAT-2 is a novel SH2 domain-containing protein that is up-regulated by Ewing's sarcoma *EWS/FLI1* fusion gene. *Oncogene*, *13*: 2649–2658, 1996.
25. Arvand, A., Bastians, H., Welford, S. M., Thompson, A. D., Ruderman, J. V., and Denny, C. T. EWS/FLI1 up-regulates mE2-C, a cyclin-selective ubiquitin conjugating enzyme involved in cyclin B destruction. *Oncogene*, *17*: 2039–2045, 1998.
26. Ohno, T., Rao, V. N., and Reddy, E. S. EWS/Fli-1 chimeric protein is a transcriptional activator. *Cancer Res.*, *53*: 5859–5863, 1993.
27. Graves, B. J., and Petersen, J. M. Specificity within the ets family of transcription factors. *Adv. Cancer Res.*, *75*: 1–55, 1998.
28. Fitzsimmons, D., Hodsdon, W., Wheat, W., Maira, S. M., Wasyluk, B., and Hagman, J. Pax-5 (BSAP) recruits *Ets* proto-oncogene family proteins to form functional ternary complexes on a B-cell-specific promoter. *Genes Dev.*, *10*: 2198–2211, 1996.
29. Goetz, T. L., Gu, T. L., Speck, N. A., and Graves, B. J. Auto-inhibition of Ets-1 is counteracted by DNA binding cooperativity with core-binding factor  $\alpha 2$ . *Mol. Cell. Biol.*, *20*: 81–90, 2000.
30. Rao, V. N., Ohno, T., Prasad, D. D., Bhattacharya, G., and Reddy, E. S. Analysis of the DNA-binding and transcriptional activation functions of human Fli-1 protein. *Oncogene*, *8*: 2167–2173, 1993.
31. Tamayo, P., Slonim, D., Mesirov, J., Zhu, Q., Kitareewan, S., Dmitrovsky, E., Lander, E. S., and Golub, T. R. Interpreting patterns of gene expression with self-organizing maps: methods and application to hematopoietic differentiation. *Proc. Natl. Acad. Sci. USA*, *96*: 2907–2912, 1999.
32. Coller, H. A., Grandori, C., Tamayo, P., Colbert, T., Lander, E. S., Eisenman, R. N., and Golub, T. R. Expression analysis with oligonucleotide microarrays reveals that MYC regulates genes involved in growth, cell cycle, signaling, and adhesion. *Proc. Natl. Acad. Sci. USA*, *97*: 3260–3265, 2000.